

TOPICAL REVIEW • OPEN ACCESS


Charge exchange of slow highly charged ions from an electron beam ion trap with surfaces and 2D materials

To cite this article: A Niggas *et al* 2024 *J. Phys. B: At. Mol. Opt. Phys.* **57** 072001

View the [article online](#) for updates and enhancements.

You may also like

- [Optimization of the electron beam properties of Dresden EBIT devices for charge breeding](#)
A Thorn, E Ritter, A Sokolov et al.
- [Room-temperature EBIS/T developments: past, present and future](#)
V P Ovsyannikov and G Zschornack
- [The physics program at the Kielce EBIS-A facility](#)
D Bana, J Braziewicz, J Semaniak et al.

The logo for kiutra, featuring a stylized circular icon to the left of the word "kiutra" in a lowercase, sans-serif font.A photograph of a Kiutra cryogenic solution, showing a vertical column with a sample stage and a control panel at the base.

Easy-to-use and Helium-3 free
cryogenics solutions

LEARN MORE

Topical Review

Charge exchange of slow highly charged ions from an electron beam ion trap with surfaces and 2D materials

A Niggas* , M Werl , F Aumayr  and R A Wilhelm* 

TU Wien, Institute of Applied Physics, Vienna, Austria

E-mail: anna@iap.tuwien.ac.at and wilhelm@iap.tuwien.ac.at

Received 15 September 2023, revised 7 January 2024

Accepted for publication 28 February 2024

Published 18 March 2024



CrossMark

Abstract

Electron beam ion traps allow studies of slow highly charged ion transmission through freestanding 2D materials as an universal testbed for surface science under extreme conditions. Here we review recent studies on charge exchange of highly charged ions in 2D materials. Since the interaction time with these atomically thin materials is limited to only a few femtoseconds, an indirect timing information will be gained. We will therefore discuss the interaction separated in three participating time regimes: energy deposition (charge exchange), energy release (secondary particle emission), and energy retention (material modification).

Keywords: highly charged ions, ion beam spectroscopy, electron emission, charge exchange, nanostructuring, 2D materials

1. Introduction

While photons and electrons can be tuned in terms of their kinetic energy, using ions brings one additional degree of freedom: the charge state of the projectile. By ionising more and more electrons from an atom, its potential energy, i.e. the binding energy of all missing electrons, can reach several tens of keV. The potential energy of these highly charged ions (HCIs) increases quickly with charge state, e.g. for low charge states $q = 1, 2$, xenon only possesses a potential energy on the order of ~ 10 eV. For fully ionised xenon it can reach more than 200 keV [1]. Using such projectiles in ion-interaction studies

thus introduces a new regime of processes triggered by deposition of this potential energy rather than solely by the kinetic energy of the projectile.

In the last decades there has been enormous progress in development of sources for HCIs [2–9]. Most of them rely on subsequent removal of electrons via electron impact ionisation processes [10] that require trapping the ions until they have reached their final charge state. Examples for these sources are electron cyclotron resonance ion sources (ECRIS), where electrons are heated via microwave injection to ionise atoms/ions trapped in a magnetic bottle [11] and electron beam ion traps/sources (EBIT/EBIS) [12]. In the latter a high-density electron beam collides with gas atoms placed in a set of drift tubes forming the ion trap.

The simple availability of highly charged ions has also driven possible applications. Besides studies examining their usability for atomic clocks [13, 14], they are industrially used for extreme ultraviolet (EUV) light production necessary for nanolithography [15, 16]. HCIs can also be used to create nanostructures in materials [17]. However, to be in full

* Authors to whom any correspondence should be addressed.



Original Content from this work may be used under the terms of the [Creative Commons Attribution 4.0 licence](https://creativecommons.org/licenses/by/4.0/). Any further distribution of this work must maintain attribution to the author(s) and the title of the work, journal citation and DOI.

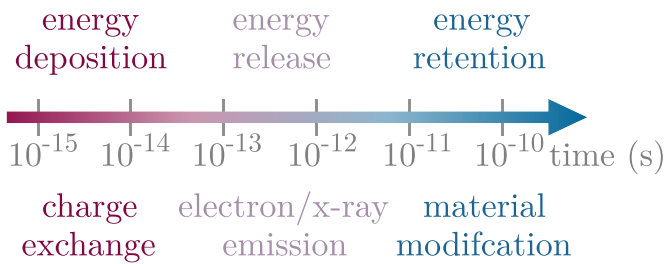


Figure 1. Timeline of (highly charged) ion interaction with a material.

control of their possibilities for nanostructuring of materials, it is important to understand the underlying mechanisms. Only then one will be able to systematically tune parameters such as ion species, kinetic energy and charge as well as irradiation geometry and sample temperature conditions in order to create some intended structures. For this, it is necessary to extract HCIs from the source, which is done not only at big research facilities like at GSI Darmstadt [18], the Multicharged Ion Research Facility (MIRF) at Oak Ridge National Laboratory [19], the Heavy Ion Research Facility in Lanzhou (HIRFL) [20] or at the High-Intensity heavy-ion Accelerator Facility (HIAF) in Huizhou (China) [21], but also in lab-size EBITs: The ions then can be directed towards gas [22–26] or solid targets [27–31] and HCI interaction with other molecules and solids can be studied. For the latter, a multitude of data has been achieved using bulk materials, focusing, e.g. on charge exchange and potential energy deposition [29, 32–34], secondary particle emission like x-rays [35–42], electrons [43–51] or sputtered target atoms [52–60], or nanostructuring [17, 30, 61–63].

In recent years, following the discovery of stable 2D materials, new insights could be gained: Using these ultimately thin surface-only samples, the interaction of HCIs with a sample can be limited to a well-defined area. This allows the exclusion of sub-surface secondary interaction contributions from measured results and thus renders studying the primary interaction of an HCI impacting on a material surface possible.

Beyond that, the limited sample thickness also restricts the interaction time to a few femtoseconds. This allows indirect access to timing information of HCI-solid interactions, which are summarised in the timeline shown in figure 1: Primary ion impact and energy deposition happen within femtoseconds, followed by energy release, e.g. in the form of emission of secondary particles. Finally, energy retention leads to permanent material modification.

Within this work we will review the interaction of highly charged ions with 2D materials with regard to these time regimes. The three main chapters will focus on charge exchange, secondary particle emission, and nanostructuring. In this context, we will discuss why HCIs are an ideal tool to study ultra-fast processes on a nanoscale.

2. Methods

Studying freestanding 2D materials brings many challenges, as in contrast to bulk materials, a defect in the layer might expose atoms of a completely different support substrate. This can distort experimental results. Hence, it is necessary to make sure to exclude unwanted contributions in experimental scattering or emission spectra and to focus on the material layer itself. One method to do this, is to perform coincidence measurements between a quantity of interest on the one hand, and a quantity that allows separation of 2D and support layers on the other.

At TU Wien, for example, we employ a Dreebit EBIS-A [64] with three drift tubes operated at room temperature and a miniaturised EBIS-C1 from D.I.S Germany GmbH [65]. Using electrostatic extraction optics, HCIs are guided from the source towards an ion spectrometer discussed in detail in [66]. It hosts a multichannel plate (MCP) detector allowing to detect the HCIs after interacting with samples. In addition to that, we use two electron detectors: a passivated implanted planar silicon (PIPS) detector biased at ~ 30 kV placed behind an extraction grid of a few hundred Volts and an electrostatic hemispherical energy analyser (HEA). The former is used for electron emission statistics measurements, i.e. to measure the total number of emitted electrons per incident ion [67] and the HEA to determine the electron energy distribution [68]. The whole spectrometer is operated in a coincidence mode correlating ion and electron signals. This gives access to the ion time of flight and therefore the particles' energy loss—a quantity permitting the differentiation of 2D sample and support structures. A detailed explanation of the coincidence technique as well as its application can be found in [69, 70]. Similar setups (with and without coincidence options) are also used in [71–77], where some also include x-ray detectors [35, 78] or secondary neutral mass spectrometers for sputtered particles [79].

3. HCI-surface interaction

Before going into detail let us review the general current understanding about HCI-solid interaction:

An HCI with its high potential energy influences the electronic landscape of a sample while it is approaching. According to the classical over-the-barrier model proposed by Burgdörfer *et al* [80], one can estimate that several Å above the surface there is a critical distance r_c at which a resonant and classically allowed electron transfer (over the barrier) leads to a population of the projectile's high n -shells. This forms a hollow atom [81, 82], where $n \sim q$, the initial ion charge state [80]. While further approaching the surface, this hollow atom starts to de-excite via radiative and non-radiative channels. The ultra-fast de-excitation measured in experiments [32, 33, 83, 84] presented a bottleneck problem for a long time, since it could not be explained by decay rates of common mechanisms like Auger–Meitner neutralisation, autoionisation or sidefeeding [85]. Only recently the interatomic

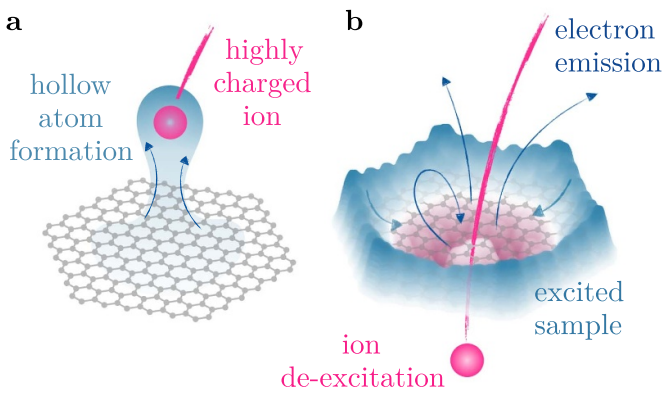


Figure 2. Schematic representation of the interaction of a highly charged ion with a 2D material. (a) Shows the hollow atom formation, which sets in via resonant electron transfer several Å above the sample. (b) After interacting with the material, e.g. capturing electrons as well as emitting electrons from the sample, the de-excited ion leaves the material in a much lower charge state. Reprinted figure with permission from [68], Copyright (2022) by the American Physical Society.

Coulombic decay (ICD) [86–91] was proposed to be the dominant process in the de-excitation of HCIs [85]: Within this two-center Auger–Meitner process (related to Auger–Meitner deexcitation [92]), the hollow atom’s de-excitation energy is transferred to the sample. This can lead to the emission of electrons or also to material modification. A schematic of the chronology of the interaction of a HCI with a sample surfaces is depicted in figure 2.

3.1. Energy deposition: charge exchange

As already discussed by Niels Bohr over a century ago [93], particles traveling in a material accommodate to an equilibrium charge state defined by balanced electron capture and loss cross sections. For slow highly charged ions, with velocities v smaller than the Bohr velocity v_0 , this equilibrium charge state is $q_{eq} \rightarrow 0$. Reaching this equilibrium charge marks the first part of the HCI–solid interaction shown in figure 1, namely charge exchange and energy deposition.

However, using thick bulk samples restricts access to the ion charge state after the impact, except one uses special geometries like grazing incidence scattering [32, 94]. This challenge may be overcome by studying thin foils or the thinnest possible solid samples, 2D materials. For these samples, projectiles can be detected after the interaction in a transmission geometry.

Experiments with thin foils (and fast projectiles) already indicated that the equilibrium charge state is reached within only a few layers of material thickness [33, 83]. Studies with freestanding carbon nano membranes (CNMs) [95] and single-layer graphene (SLG) [96] were conducted to perform a systematic investigation of charge neutralisation times in a material. Figure 3(a) shows an exemplary spectrum of 130 keV Xe^{30+} ions transmitted through SLG. Three different areas can be distinguished:

- (i) There is a fraction of ions transmitting through cracks/uncovered areas of the sample leading to random coincidences. These particles impinge on the detector with the initial narrow angular distribution provided from the EBIT and the original charge state q_{in} of the highly charged projectile ion.
- (ii) Ions transmitting through clean sample areas will form an intermediate charge state distribution with mean value q_{sample} , which is affected by the ion parameters. E.g., the distribution shifts up/down when increasing/decreasing the projectile velocity. Scattering of the particles in the sample also leads to a broadening of the distribution in horizontal direction. An in-depth analysis of Creutzburg *et al* [97] showed that for higher scattering angles the exit charge state decreases, i.e. more electrons are captured by the projectile. This is related to the trajectory of the ion: Closer collisions lead to larger scattering angles and increased deexcitation rates and thus a smaller exit charge state.
- (iii) Some particles going through support or contaminated areas neutralise completely, i.e. $q_{support} \sim 0$. There, multiple scattering events occur, which lead to an even broader scattering distribution than in the previous case (ii).

Variation of ion velocities and charge states, respectively, showed an exponential charge decay of the form [33, 96, 98, 99]

$$n_e = q_{in} - \bar{q}_{out} = q_{in} \left(1 - e^{-\tau/\tau_n}\right), \quad (1)$$

where n_e is the number of captured electrons by the ion, q_{in} is the incident charge state, and \bar{q}_{out} is the mean exit charge state. τ is the interaction time and τ_n a charge-state-dependent neutralisation time constant. Depending on the charge state, for SLG, τ_n in the range of 1–5 fs were found [96].

A consecutive study using freestanding multilayers of graphene (bilayer graphene = BLG, trilayer graphene = TLG) is summarised in figure 3(b). We could show that by taking into account a prolonged interaction time due to an increased number of material layers, the charge exchange with 1–3 layers of graphene can be universalised: In the figure, data for three xenon charge states ($q = 20, 30, 40$) is shown for various inverse velocities $1/v$ scaled with the number of material layers n_L . The data again follows the exponential behaviour from (1) and suggests that the neutralisation depends solely on the interaction time the ion spends in close proximity to the sample [100].

As soon as porous materials come into play, another distribution occurs: Creutzburg *et al* found a fourth distribution at higher charge states by recording charge exchange patterns of highly charged ions transmitted through monolayers of MoS_2 . This distribution could be explained by the ion transmitting through nano-sized pores in the material, so that the interaction (time) with the material itself is limited. Then only a smaller amount of electrons may be stabilised (i.e. de-excite by ICD into orbitals with high binding energy preventing their peel-off or autoionisation) and higher exit charge states are found [75].

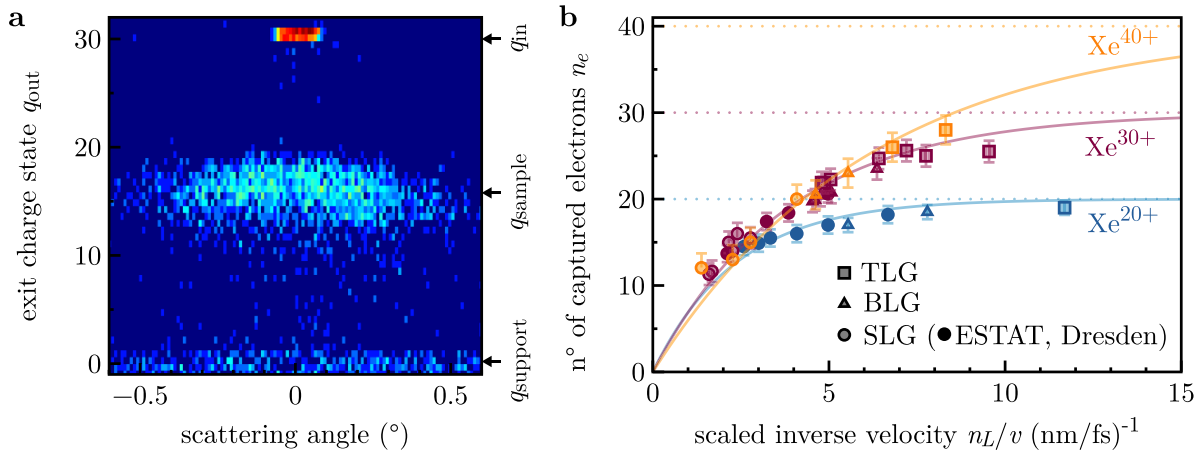


Figure 3. Charge exchange spectroscopy. (a) shows the exit charge state distribution of 130 keV Xe^{30+} transmitted through single-layer graphene (SLG). Three distinct distributions can be seen: the incident beam with charge state q_{in} , the distribution for the sample with $\bar{q}_{\text{sample}} \sim 15.7$ and the support structure $\bar{q}_{\text{support}} \sim 0$. In (b) the number of captured electrons $n_e = q_{\text{in}} - q_{\text{out}}$ is given in dependence of the inverse projectile velocity v scaled with the number of material layers n_L : data for SLG, bilayer graphene (BLG) and trilayer graphene (TLG) show a universal exponential behaviour for each incident charge state Xe^{q+} for $q = \{20, 30, 40\}$. Adapted from [100]. CC BY 4.0.

Similar results were discussed in [95] for CNMs. This effect, which is very sensitive to the sample structure, was discussed as possible analysis technique for material textures [101].

The first stage of the interaction of HCIs with solids is dominated by ultrafast electron transfer from the target material to the projectile and a subsequent deexcitation of the ion stabilising the captured electrons. Since this deexcitation of the HCI goes hand in hand with the deposition of its potential energy within the material, a lot of energy is pumped into the electronic system of the target in a short time (\sim fs). Additionally, Wilhelm *et al* could even find an increased kinetic energy loss with increasing charge exchange [95], further increasing the amount of excitation energy in the material. Several release mechanisms are possible for the material to relax after this excitation, which will be covered in the following sections.

3.2. Energy release: secondary particle emission

Common energy release mechanisms cover the translation of excitation energy to the emission of (possible high-energetic) secondary particles, i.e. electrons, sputtered target atoms and x-rays. For the latter two, there exist many literature data for studies including bulk samples, however, only scarce information is available for HCI interaction with (freestanding) 2D materials. There is solely a study by Skopinski *et al* using MoS_2 layers on Au(111) substrate revealing that sputtered Mo atoms by highly charged xenon ions have energies on the order of only 1 eV [102].

For the emission of x-rays, experiments with argon as well as xenon on SLG were performed [103]. In the case of argon, H-like ($q = 17$) as well as bare ($q = 18$) projectiles were used. In general the spectra are very well comparable to literature data on bulk surfaces with similar K_α to K_β intensity ratios [104, 105]. In the case of bare argon, due to two vacancies in the $n = 1$ shell, additional hypersatellite lines (both K_α and K_β) were measured. Their relative intensity is higher

than the satellite line, implying that the first vacancy is filled ($1s^0 \rightarrow 1s^1$) faster than the second, remaining vacancy ($1s^1 \rightarrow 1s^2$). Using xenon ions ($22 \leq q \leq 35$) showed another interesting observation: Increasing the number of vacancies in the M-shell leads to a linear shift towards higher energies for the emitted x-rays from the $4f \rightarrow 3d$ -transition resulting from the de-excitation. This was attributed to the fact that the average number of spectator electrons at the time of the transition decreases [106].

First experiments regarding the electron emission from freestanding SLG were performed by Schweska *et al* [107]. They could show that (depending on the kinetic energy) up to 100 electrons are being emitted by a single HCI impact (with a charge state of $q = 40$). A majority of these electrons have energies well below 15 eV, which is in good agreement with the proposed deexcitation scheme in [85]. The interatomic Coulombic decay, namely, suggests that many low-energy electrons should be emitted within the deexcitation cascade of the HCI. Follow-up experiments published in [68] confirmed this finding of mainly low-energy electrons with complex coincidence measurements of the electron energy distribution using a hemispherical energy analyser in addition to the retarding field analysis performed in [107].

By comparing the electron yields of graphene and MoS_2 , we could also demonstrate that the high yield found for graphene in [107] is strongly dependent on the specific material used: Under the same conditions the electron yield of semi-conducting MoS_2 amounts to only 1/6 when compared to SLG (cf figure 4). This was explained qualitatively using a charge patch building up in the material layer which stays longer in MoS_2 than in graphene due to the electronic material properties. This hinders low-energy electrons from escaping the material in MoS_2 leading to a reduced measured yield, especially in the low-energy regime [68]. Calculations were performed based on a model presented in [108] to investigate the charge carrier dynamics quantitatively in a

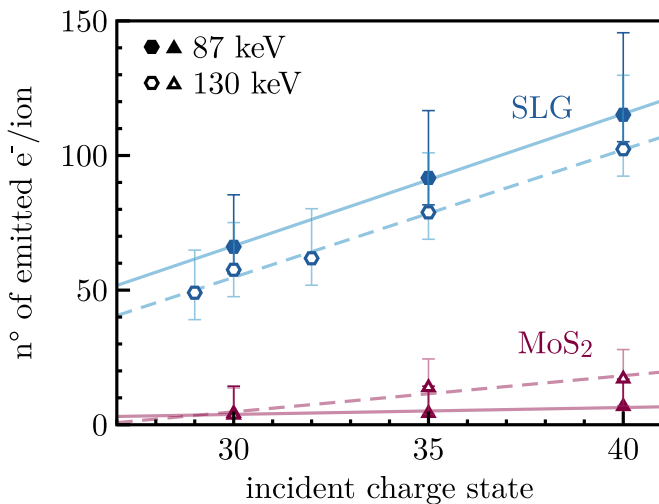


Figure 4. Electron yield from monolayers of graphene and MoS₂ induced by highly charged Xe ions. Reprinted figure with permission from [68], Copyright (2022) by the American Physical Society.

graphene and MoS₂ layer upon HCI impact, respectively. Results showed that even in the semiconductor the charge dissipates within \sim fs, which demonstrates electron emission to be prompt upon HCI impact and strongly influenced by the charge dynamics in the material. Studying electron emission can thus give access to ultrafast carrier dynamics in a probed material.

To conclude this second phase of ion–solid interaction: The deexcitation of the hollow atom formed in step 1 (charge exchange discussed in section 3.1) and the accompanying potential energy deposition may trigger the emission of secondary particles through either sputtering [102], radiative decay [103] or non-radiative decay [68, 107].

3.3. Energy retention: material modification

Another release mechanism of deposited energy besides the emission of secondary particles is the permanent modification of the material due to energy retention. For bulk samples, when exceeding material-specific threshold combinations of kinetic and potential particle energies [30], a formation of hillocks or pits could be observed [30, 61–63, 109]. However, most studies focused on semiconducting and insulating materials, as for metals only few experiments showed successful nanostructuring using slow highly charged ions [110, 111]. As an explanation for this behaviour one typically uses charge mobilities in the respective materials: While in metals the deposited energy can be dissipated very fast, in semiconductors and insulators a confinement of the energy around the impact position leads to a translation of the excitation energy to the lattice system and further on to the formation of nanostructures. Only recently, experiments with gold nanoislands [60] and nanolayers [112] could demonstrate that in these limited volumes material modifications induced by HCI impact becomes possible.

A similar behaviour was documented for ultrathin and two-dimensional materials: On the one hand, Gruber *et al* irradiated freestanding layers of graphene with HCIs, a semimetal, without producing any damage [96]. Note that for graphene layers placed on a substrate HCI-induced defects were discussed in [113, 114] and for MoS₂ in [115]. On the other hand, Kozubek *et al* irradiated semiconducting freestanding MoS₂ layers with slow highly charged xenon ions. Using transmission electron microscopy they located ion-induced nanometre-sized pores. Just like for hillocks and craters in bulk materials, also the pore size in the MoS₂ layer increases with increasing potential energy [116]. A similar behaviour was already found, prior to these experiments with 2D materials, using 1 nm thick carbon nano membranes. In these insulating layers, found pore diameters were even larger and tunable using the projectile potential energy up to 15 nm [117].

These experiments showed a clear trend that nanoscale material modification depends on the electronic properties of the investigated material. Creutzburg *et al* tested this hypothesis by fluorisation of single-layer graphene, which makes the material insulating. Indeed, thereby the material becomes susceptible to pore formation using HCIs [118].

In [119], we combined the findings discussed above—both in terms of pore formation susceptibility and neutralisation times—using van der Waals heterostructures: A stack of monolayers of graphene and MoS₂ was irradiated with HCIs, where the result strongly depends on the orientation of the material layers. If MoS₂ faces the ion beam first, pores can be located in the MoS₂ layer using a transmission microscopy afterwards (cf figure 5). The other way round, irradiating the graphene layer first, yields no pores in the MoS₂ layer. As the ion deposits almost 90% of its potential energy within the very first material layer, the graphene layer on top acts as a shield preventing the MoS₂ layer beneath from getting damaged. This surface sensitivity was also strengthened by experiments using up to three layers MoS₂ on graphene, where HCI-induced pores could only be found in the first two layers (with a decreased pore diameter for the second material layer). This emphasises the suitability of highly charged ions for material modification [120].

In summary, this final phase of the electronically-driven material modification is characterised by bond weakening due to excitations and atom removal by either Coulomb repulsion (charged surface atoms, high kinetic energy release) or desorption (neutral surface atoms, hyperthermal energies).

4. Theoretical modelling

Besides the experimental work summarised in the previous sections, a lot of effort was also put in finding theoretical descriptions to model the processes discussed above. Both empiric models as well as first principles models were used to try and describe the energy loss and charge exchange of the ions as well as the effect on the target material.

Guo *et al* [121] proposed a semi-classical model allowing to study energy loss and charge exchange of slow highly charged

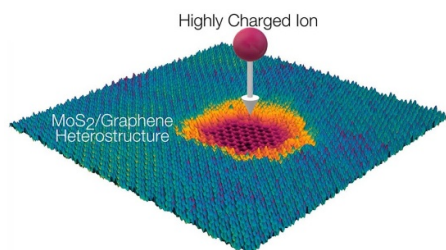


Figure 5. Nanostructure formation using highly charged ions. Van der Waals stack of an MoS₂ monolayer on top of single-layer graphene. After impact of 170 keV Xe³⁸⁺ a pore is visible in MoS₂ with graphene being still intact beneath. Reprinted with permission from [119]. Copyright (2020) American Chemical Society.

ions in ultrathin materials based on the over-the-barrier model and Lindhard formula.

Rainbow scattering, the classical 2D scatter pattern of highly charged ions in thin foils, was first discussed by Petrović *et al* [122] and then for graphene with proton projectiles by Ćosić *et al* [123].

In terms of first principles approaches, the GPAW package [124–127] is a time-dependent density functional theory (TDDFT) approach using the Ehrenfest dynamics scheme. It has been successfully applied to model energy transfer of low-charged ions while transmitting through 2D materials [128] and should be, in principal, applicable also to highly charged ions (at least with empty subshells). The same applies to other TDDFT approaches [129, 130].

However, TDDFT does not include any electronic transitions, e.g. inter- or intraatomic Auger–Meitner processes like ICD. To take that into account Wilhelm and Grande prepared the simulation package TDPot (Time-Dependent Potential) [131], which randomly chooses impact parameters in the 2D lattice. The deexcitation is subsequently modelled with the interatomic Coulombic decay using either extrapolated interatomic-distance-dependent experimental rates [131] or *ab-initio* calculated rates for the system of multiply charged ions transmitted through graphene [100]. The inclusion of these additional effects allows to more accurately describe the final ion charge state after the interaction. The model was effectively tested for xenon ions interacting with freestanding layers of graphene and MoS₂ [75].

Charge-exchange and neutralisation is also included in the Green function approach hopping model prepared by Balzer and Bonitz [108], which shows good agreement with graphene transmission experiments. The model was further extended to simulate the charge dissipation in the material after the HCI impact to understand the influence on electron emission [68].

A related approach was taken by Grosseck *et al* [132], who also introduce an excitation in a 2D material to mimic an HCI-impact: Here, a honeycomb lattice with graphene lattice constant is used, but other materials can be addressed using adjusted hopping times. A relaxation of the material is analysed, where atoms with kinetic energies above their binding energy are assumed to be emitted from the material. Therewith, pore

formation susceptibilities of 2D materials with different electronic properties can be examined. Finally, Kozubek *et al* [133] further applied the two-temperature model to HCI-induced pores in hexagonal boron nitride, which showed good agreement with experimental results achieved using hBN samples on various substrates.

5. Conclusion and outlook

The results discussed above summarise how slow highly charged ion transmission experiments through freestanding 2D materials can be used to unravel time dynamics of ion–solid interaction. Transmission times are limited to only femtoseconds, nevertheless, almost complete neutralisation can be observed depending on charge state/velocity combinations. Neutralisation times on the order of femtoseconds could thus be derived. Following the ion impact, secondary particles are being emitted. So far, focus was laid on studying electron emission, which was found to happen prompt after the ion hits the material. On the long term, energy retention leads to modification of the material, i.e. nanopore formation in the case of monolayers. There, a strong dependence of the pore formation susceptibility of a material on its electronic properties could be observed: In experiments with xenon ions up to charge states of $q = 40$, pores were introduced in semiconducting and insulating layers but not in semimetals. Simulations, however, predict also pore formation in the latter, for the case of very high charge states and potential energies, respectively. These charge states exceed current possibilities of experiments with EBITs. Great efforts are currently being made to make these measurement parameters available in the future, e.g. at GSI Darmstadt, where the S-EBITs as well as the HITRAP facility with a complex deceleration system shall be able to produce slow ions up to bare uranium [18].

Data availability statement

The data that support the findings of this study are available upon reasonable request from the authors.

Acknowledgments

The authors acknowledge funding from the Austrian Science Fund (FWF) within the projects 10.55776/Y1174, 10.55776/I4914 and 10.55776/P36264.

ORCID iDs

A Niggas  <https://orcid.org/0000-0002-5838-5789>

M Werl  <https://orcid.org/0000-0003-2280-6112>

F Aumayr  <https://orcid.org/0000-0002-9788-0934>

R A Wilhelm  <https://orcid.org/0000-0001-9451-5440>

References

- [1] DREEBIT | Ion Beam Technology 2023 *Ionization Energy Database* (available at: www.dreebit-ibt.com/ionization-energy-database.html)
- [2] Gillaspay J D 2001 *J. Phys. B: At. Mol. Opt. Phys.* **34** R93
- [3] Sortais P 1995 *Nucl. Instrum. Methods Phys. Res. B* **98** 508–16
- [4] Hitz D, Girard A, Serebrennikov K, Melin G, Cormier D, Mathonnet J M, Chartier J, Sun L, Briand J P and Benhachoum M 2004 *Rev. Sci. Instrum.* **75** 1403–6
- [5] Zhao H, Sun L, Guo J, Lu W, Xie D, Hitz D, Zhang X and Yang Y 2017 *Phys. Rev. Accel. Beams* **20** 094801
- [6] Xie Z Q 1998 *Rev. Sci. Instrum.* **69** 625–30
- [7] Douysset G, Khodja H, Girard A and Briand J P 2000 *Phys. Rev. E* **61** 3015–22
- [8] Zhao H Y, Zhang J J, Jin Q Y, Liu W, Wang G C, Sun L T, Zhang X Z and Zhao H W 2016 *Rev. Sci. Instrum.* **87** 02A917
- [9] Short R T, O C-S, Levin J C, Sellin I A, Liljeby L, Hultd S, Johansson S E, Nilsson E and Church D A 1986 *Phys. Rev. Lett.* **56** 2614–7
- [10] Donets E D 1983 *Phys. Scr.* **T3** 11–18
- [11] Geller R 1990 *Annu. Rev. Nucl. Part. Sci.* **40** 15
- [12] Zschornack G, Kreller M, Ovsyannikov V, Grossman F, Kentsch U, Schmidt M, Ullmann F and Heller R 2008 *Rev. Sci. Instrum.* **79** 02A703
- [13] King S A *et al* 2022 *Nature* **611** 43–47
- [14] Kozlov M, Safronova M, Crespo López-Urrutia J and Schmidt P 2018 *Rev. Mod. Phys.* **90** 045005
- [15] Versolato O O 2019 *Plasma Sources Sci. Technol.* **28** 083001
- [16] Scheers J *et al* 2020 *Phys. Rev. A* **101** 062511
- [17] Aumayr F, Facsko S, El-Said A, Trautmann C and Schleberger M 2011 *J. Phys.: Condens. Matter* **23** 393001
- [18] Trotsenko S *et al* 2015 *GSI Scientific Report* 2014 (GSI Helmholtzzentrum für Schwerionenforschung) (available at: <https://repository.gsi.de/record/183977>)
- [19] Meyer F *et al* 2006 *Nucl. Instrum. Methods Phys. Res. B* **242** 71–78
- [20] Mao L *et al* 2020 *J. Instrum.* **15** T12015
- [21] Zhou X and Yang J (the HIAF project team) 2022 *AAPPS Bull.* **32** 35
- [22] Barat M and Roncin P 1992 *J. Phys. B: At. Mol. Opt. Phys.* **25** 2205–43
- [23] Knudsen H, Haugen H K and Hvelplund P 1981 *Phys. Rev. A* **23** 597–610
- [24] Siddiki M A K A, Nrisimhamurthy M, Kumar K, Mukherjee J, Tribedi L C, Khan A and Misra D 2022 *Rev. Sci. Instrum.* **93** 113313
- [25] Allen F I, Biedermann C, Radtke R and Fussmann G 2006 *Rev. Sci. Instrum.* **77** 03B903
- [26] Stolterfoht N, Platten H, Schiwietz G, Schneider D, Gulyás L, Fainstein P D and Salin A 1995 *Phys. Rev. A* **52** 3796–802
- [27] Arnau A *et al* 1997 *Surf. Sci. Rep.* **27** 113–239
- [28] Schenkel T, Hamza A V, Barnes A V, Schneider D H, Banks J C and Doyle B L 1998 *Phys. Rev. Lett.* **81** 2590–3
- [29] Meyer F W, Overbury S H, Havener C C, Van Emmichoven P A Z and Zehner D M 1991 *Phys. Rev. Lett.* **67** 723–6
- [30] El-Said A S, Wilhelm R A, Heller R, Facsko S, Lemell C, Wachter G, Burgdörfer J, Ritter R and Aumayr F 2012 *Phys. Rev. Lett.* **109** 117602
- [31] Wilhelm R A 2022 *Surf. Sci. Rep.* **77** 100577
- [32] Winecki S, Cocke C L, Fry D and Stöckli M P 1996 *Phys. Rev. A* **53** 4228–37
- [33] Hattass M, Schenkel T, Hamza A V, Barnes A V, Newman M W, McDonald J W, Niedermayr T R, Machicoane G A and Schneider D H 1999 *Phys. Rev. Lett.* **82** 4795–8
- [34] Schenkel T, Barnes A V, Niedermayr T R, Hattass M, Newman M W, Machicoane G A, McDonald J W, Hamza A V and Schneider D H 1999 *Phys. Rev. Lett.* **83** 4273–6
- [35] Jablonski L, Banaa D, Jagodzinski P, Kubala-Kukus A, Sobota D, Stabrawa I, Szary K and Pajek M 2023 *X-ray Spectrom.* **52** xrs.3381
- [36] Jablonski L, Banas D, Braziewicz J, Czub J, Jagodzinski P, Kubala-Kukus A, Sobota D, Stabrawa I and Pajek M 2017 *J. Phys.: Conf. Ser.* **810** 012050
- [37] Beiersdorfer P, Olson R E, Brown G V, Chen H, Harris C L, Neill P A, Schweikhard L, Utter S B and Widmann K 2000 *Phys. Rev. Lett.* **85** 5090–3
- [38] Liang G Y, Zhu X L, Wei H G, Yuan D W, Zhong J Y, Wu Y, Hutton R, Cui W, Ma X W and Zhao G 2021 *Mon. Not. R. Astron. Soc.* **508** 2194–203
- [39] Perez J A, Olson R E and Beiersdorfer P 2001 *J. Phys. B: At. Mol. Opt. Phys.* **34** 3063–72
- [40] Cumbee R S, Mullen P D, Lyons D, Shelton R L, Fogle M, Schultz D R and Stancil P C 2017 *Astrophys. J.* **852** 7
- [41] Schulz M, Cocke C L, Hagmann S, Stöckli M and Schmidt-Böcking H 1991 *Phys. Rev. A* **44** 1653–8
- [42] Dergham P, Aumayr F, Lamour E, Macé S, Prigent C, Steydli S, Vernhet D, Werl M, Wilhelm R A and Trassinelli M 2022 *Atoms* **10** 151
- [43] Bodewits E, Hoekstra R, Dobes K and Aumayr F 2014 *Phys. Rev. A* **90** 052703
- [44] Bodewits E, Hoekstra R, Kowarik G, Dobes K and Aumayr F 2011 *Phys. Rev. A* **84** 042901
- [45] Aumayr F and Winter H 2007 Potential electron emission from metal and insulator surfaces *In: Slow Heavy-Particle Induced Electron Emission from Solid Surfaces (Springer Tracts in Modern Physics vol 225)* (Springer) p 79
- [46] Kurz H, Aumayr F, Lemell C, Töglhofer K and Winter H 1993 *Phys. Rev. A* **48** 2182–91
- [47] Kurz H, Aumayr F, Winter H, Schneider D, Briere M and McDonald J 1994 *Phys. Rev. A* **49** 4693
- [48] Köhrbrück R, Sommer K, Biersack J P, Bleck-Neuhaus J, Schippers S, Roncin P, Lecler D, Fremont F and Stolterfoht N 1992 *Phys. Rev. A* **45** 4653–60
- [49] Limburg J, Das J, Schippers S, Hoekstra R and Morgenstern R 1994 *Phys. Rev. Lett.* **73** 786–9
- [50] Köhrbrück R, Stolterfoht N, Schippers S, Hustedt S, Heiland W, Lecler D, Kemmler J and Bleck-Neuhaus J 1993 *Phys. Rev. A* **48** 3731–40
- [51] Schippers S, Hustedt S, Heiland W, Köhrbrück R, Bleck-Neuhaus J, Kemmler J, Lecler D and Stolterfoht N 1992 *Phys. Rev. A* **46** 4003–11
- [52] Hayderer G, Cernusca S, Hoffmann V, Niemann D, Stolterfoht N, Schmid M, Varga P, Winter H and Aumayr F 2001 *Nucl. Instrum. Methods Phys. Res. B* **182** 143–7
- [53] Schenkel T, Briere M A, Schmidt-Böcking H, Bethge K and Schneider D H 1997 *Phys. Rev. Lett.* **78** 2481–4
- [54] Hayderer G *et al* 2001 *Phys. Rev. Lett.* **86** 3530–3
- [55] Sporn M, Libiseller G, Neidhart T, Schmid M, Aumayr F, Winter H, Varga P, Grether M, Niemann D and Stolterfoht N 1997 *Phys. Rev. Lett.* **79** 945–8

- [56] Sigmund P 1969 *Phys. Rev.* **184** 383–416
- [57] Sigmund P and Claussen C 1981 *J. Appl. Phys.* **52** 990–3
- [58] Aumayr F and Winter H 2004 *Phil. Trans. R. Soc. A* **362** 77
- [59] Szabo P S *et al* 2020 *Astrophys. J.* **891** 100
- [60] Szabo G L *et al* 2023 *Small* **19** 2207263
- [61] Ritter R 2013 Nanostructures formed on surfaces due to the impact of slow highly charged ions *PhD Thesis* TU Wien, Vienna, Austria
- [62] Facsko S, Meissl W, Heller R, Wilhelm R, El-Said A S, Kowarik G, Ritter R and Aumayr F 2009 *J. Phys.: Conf. Ser.* **194** 012060
- [63] El-Said A S, Wilhelm R A, Heller R, Ritter R, Wachter G, Facsko S, Lemell C, Burgdörfer J and Aumayr F 2014 *J. Phys.: Conf. Ser.* **488** 012002
- [64] DREEBIT Ion Beam Technology 2023 *Dresden EBIS-A* (available at: <http://www.dreebit-ibt.com/product/dresden-ebis-a.html>)
- [65] DIS Germany GmbH 2024 (available at: www.dis-eng.de)
- [66] Schwestka J, Melinc D, Heller R, Niggas A, Leonhartsberger L, Winter H, Facsko S, Aumayr F and Wilhelm R 2018 *Rev. Sci. Instrum.* **89** 085101
- [67] Lemell C, Stöckl J, Winter H and Aumayr F 1999 *Rev. Sci. Instrum.* **70** 1653–7
- [68] Niggas A *et al* 2022 *Phys. Rev. Lett.* **129** 086802
- [69] Niggas A, Schwestka J, Weichselbaum D, Heller R, Aumayr F and Wilhelm R A 2022 Coincidence technique to study ion-induced electron emission from atomically thin materials *Proc. SPIE* **12131** 121310H
- [70] Niggas A, Schwestka J, Creutzburg S, Gupta T, Eder D, Bayer B C, Aumayr F and Wilhelm R A 2020 *J. Chem. Phys.* **153** 014702
- [71] Barat M, Gaboriaud M N, Guillemot L, Roncin P, Laurent H and Andriamonje S 1987 *J. Phys. B: At. Mol. Phys.* **20** 5771–83
- [72] Morosov V, Gaboriaud M, Barat M and Roncin P 1997 *Nucl. Instrum. Methods Phys. Res. B* **125** 167–9
- [73] Xu Z F *et al* 2008 *Chin. Phys. C* **32** 247–50 (available at: <http://cpc.ihep.ac.cn/fileZGWLC/journal/article/zgwlc/2008/S2/PDF/HWL2008-66.pdf>)
- [74] Wang Y Y, Zhao Y T, Sun J R, Li D H, Li J Y, Wang P Z and Xiao G Q 2011 *Chin. Phys. Lett.* **28** 053402
- [75] Creutzburg S *et al* 2020 *Phys. Rev. B* **102** 045408
- [76] Wilhelm R A, Gruber E, Smejkal V, Facsko S and Aumayr F 2016 *Phys. Rev. A* **93** 052708
- [77] Winter H 2014 *Surf. Interface Anal.* **46** 1137–42
- [78] Gumberidze A *et al* 2010 *Rev. Sci. Instrum.* **81** 033303
- [79] Skopinski L *et al* 2021 *Rev. Sci. Instrum.* **92** 023909
- [80] Burgdörfer J, Lerner P and Meyer F W 1991 *Phys. Rev. A* **44** 5674–85
- [81] Winter H and Aumayr F 1999 *J. Phys. B: At. Mol. Opt. Phys.* **32** R39
- [82] Briand J, de Billy L, Charles P, Essabaa S, Briand P, Geller R, Desclaux J, Bliman S and Ristori C 1990 *Phys. Rev. Lett.* **65** 159
- [83] Herrmann R, Cocke C L, Ullrich J, Hagmann S, Stoeckli M and Schmidt-Boecking H 1994 *Phys. Rev. A* **50** 1435–44
- [84] Childres I, Jauregui L, Park W, Cao H and Chen Y 2013 *New Dev. Photon Mater. Res.* **1** 1–20
- [85] Wilhelm R A, Gruber E, Schwestka J, Kozubek R, Madeira T I, Marques J P, Kobus J, Krasheninnikov A V, Schleberger M and Aumayr F 2017 *Phys. Rev. Lett.* **119** 103401
- [86] Averbukh V, Müller I B and Cederbaum L S 2004 *Phys. Rev. Lett.* **93** 263002
- [87] Jahnke T *et al* 2004 *Phys. Rev. Lett.* **93** 163401
- [88] Marburger S, Kugeler O, Hergenbahn U and Möller T 2003 *Phys. Rev. Lett.* **90** 203401
- [89] Cederbaum L S, Zobeley J and Tarantelli F 1997 *Phys. Rev. Lett.* **79** 4778–81
- [90] Bande A, Gokhberg K and Cederbaum L S 2011 *J. Chem. Phys.* **135** 144112
- [91] Trinter F *et al* 2013 *Phys. Rev. Lett.* **111** 093401
- [92] Hagstrum H D 1954 *Phys. Rev.* **96** 336–65
- [93] Bohr N 1948 *The Penetration of Atomic Particles Through Matter* (Munksgaard Copenhagen)
- [94] Lemell C 2000 Coincidence measurements of highly charged ions interacting with surfaces *AIP Conf. Proc.* **500** 656–65
- [95] Wilhelm R A, Gruber E, Ritter R, Heller R, Facsko S and Aumayr F 2014 *Phys. Rev. Lett.* **112** 153201
- [96] Gruber E *et al* 2016 *Nat. Commun.* **7** 13948
- [97] Creutzburg S, Niggas A, Weichselbaum D, Grande P L, Aumayr F and Wilhelm R A 2021 *Phys. Rev. A* **104** 042806
- [98] Bohr N and Lindhard J 1954 *Electron Capture and Loss by Heavy Ions Penetrating Through Matter* (I kommission hos Munksgaard)
- [99] Brandt W, Laubert R, Mourino M and Schwarzschild A 1973 *Phys. Rev. Lett.* **30** 358
- [100] Niggas A *et al* 2021 *Commun. Phys.* **4** 180
- [101] Wilhelm R A 2020 *J. Phys.: Conf. Ser.* **1412** 062010
- [102] Skopinski L 2023 *Phys. Rev. B* **107** 075418
- [103] Schwestka J, Wilhelm R, Gruber E, Heller R, Kozubek R, Schleberger M, Facsko S and Aumayr F 2018 *Nucl. Instrum. Methods Phys. Res. B* **422** 63
- [104] Bhalla C P 1973 *Phys. Rev. A* **8** 2877–82
- [105] Mirakhmedov M 1995 *Nucl. Instrum. Methods Phys. Res. B* **98** 429–35
- [106] Schuch R, Schneider D, Knapp D A, DeWitt D, McDonald J, Chen M H, Clark M W and Marrs R E 1993 *Phys. Rev. Lett.* **70** 1073–6
- [107] Schwestka J, Niggas A, Creutzburg S, Kozubek R, Heller R, Schleberger M, Wilhelm R and Aumayr F 2019 *J. Phys. Chem. Lett.* **2019** 4805–11
- [108] Balzer K and Bonitz M 2022 *Contrib. Plasma Phys.* **62** e202100041
- [109] El-Said A S *et al* 2008 *Phys. Rev. Lett.* **100** 237601
- [110] Donnelly S E and Birtcher R C 1999 *Phil. Mag. A* **79** 133–45
- [111] Pomeroy J M, Perrella A C, Grube H and Gillaspay J D 2007 *Phys. Rev. B* **75** 241409
- [112] Stabrawa I *et al* 2023 *Vacuum* **210** 111860
- [113] Hopster J, Kozubek R, Ban-d’Etat B, Guillous S, Lebius H and Schleberger M 2014 *2D Mater.* **1** 011011
- [114] Ernst P, Kozubek R, Madauß L, Sonntag J, Lorke A and Schleberger M 2016 *Nucl. Instrum. Methods Phys. Res. B* **382** 71–75
- [115] Hopster J, Kozubek R, Krämer J, Sokolovsky V and Schleberger M 2013 *Nucl. Instrum. Methods Phys. Res. B* **317** 165–9
- [116] Kozubek R *et al* 2019 *J. Phys. Chem. Lett.* **10** 904
- [117] Wilhelm R *et al* 2015 *2D Mater.* **2** 035009
- [118] Creutzburg S *et al* 2021 *Phys. Rev. Mater.* **5** 074007
- [119] Schwestka J, Inani H, Tripathi M, Niggas A, McEvoy N, Libisch F, Aumayr F, Kotakoski J and Wilhelm R A 2020 *ACS Nano* **14** 10536–43
- [120] Schleberger M and Kotakoski J 2018 *Materials* **11** 1885
- [121] Guo X, Fu Y, Zhang X, Wang X, Chen Y and Xue J 2019 *Matter Radiat. Extremes* **4** 054401
- [122] Petrovic S, Miletic L and Neškovic N 2000 *Phys. Rev. B* **61** 184
- [123] Čosić M, Petrović S and Nešković N 2018 *Nucl. Instrum. Methods Phys. Res. B* **422** 54–62
- [124] Mortensen J J, Hansen L B and Jacobsen K W 2005 *Phys. Rev. B* **71** 035109
- [125] Enkovaara J *et al* 2010 *J. Phys.: Condens. Matter* **22** 253202

- [126] Walter M, Häkkinen H, Lehtovaara L, Puska M, Enkovaara J, Rostgaard C and Mortensen J J 2008 *J. Chem. Phys.* **128** 244101
- [127] Ojanperä A, Krasheninnikov A V and Puska M 2014 *Phys. Rev. B* **89** 035120
- [128] Brand C, Debiossac M, Susi T, Aguilon F, Kotakoski J, Roncin P and Arndt M 2019 *New J. Phys.* **21** 033004
- [129] Kononov A and Schleife A 2021 *Nano Lett.* **21** 4816–22
- [130] Vázquez H, Kononov A, Kyritsakis A, Medvedev N, Schleife A and Djurabekova F 2021 *Phys. Rev. B* **103** 224306
- [131] Wilhelm R A and Grande P L 2019 *Commun. Phys.* **2** 89
- [132] Grosseck A S, Niggas A, Wilhelm R A, Aumayr F and Lemell C 2022 *Nano Lett.* **22** 9679–84
- [133] Kozubek R, Ernst P, Herbig C, Michely T and Schleberger M 2018 *ACS Appl. Nano Mater.* **1** 3765–73